



OPEN

Collagen-coated superparamagnetic iron oxide nanoparticles as a sustainable catalyst for spirooxindole synthesis

Shima Ghanbari Azarnier, Maryam Esmkhani, Zahra Dolatkah & Shahrzad Javanshir✉

In this work, a novel magnetic organic–inorganic hybrid catalyst was fabricated by encapsulating magnetite@silica ($\text{Fe}_3\text{O}_4@\text{SiO}_2$) nanoparticles with Isinglass protein collagen (IGPC) using epichlorohydrin (ECH) as a crosslinking agent. Characterization studies of the prepared particles were accomplished by various analytical techniques specifically, Fourier transform infrared (FTIR) analysis, scanning electron microscopy (SEM), transmission electron microscopy (TEM), vibrating sample magnetometry (VSM), energy-dispersive X-ray spectroscopy (EDS), X-ray powder diffraction (XRD), thermogravimetric analysis (TGA), and Brunauer–Emmett–Teller (BET) analysis. The XRD results showed a crystalline and amorphous phase which contribute to magnetite and isinglass respectively. Moreover, the formation of the core/shell structure had been confirmed by TEM images. The synthesized $\text{Fe}_3\text{O}_4@\text{SiO}_2/\text{ECH}/\text{IG}$ was applied as a bifunctional heterogeneous catalyst in the synthesis of spirooxindole derivatives through the multicomponent reaction of isatin, malononitrile, and C-H acids which demonstrated its excellent catalytic properties. The advantages of this green approach were low catalyst loading, short reaction time, stability, and recyclability for at least four runs.

Nowadays, the use of bifunctional catalysts has become a new field to promote chemical reactions in green, and environmentally friendly pathways and processes. In order to develop new approaches that are more respectful of the environment, catalyst development strategies are now oriented towards polymers of natural origin such as polysaccharides or proteins which come from renewable resources, often biocompatible and also more biodegradable than their synthetic counterparts. Bio-based heterogeneous catalysts, prepared from renewable natural polymers, have received significant attention in recent years due to their substantial advantages such as biodegradability, stability, and recyclability. The combination of nanoparticles and biodegradable polymers can result in nano-biocomposites, which have the potential for various catalytic and environmental applications^{1–5}.

Plentiful supports have been commonly used for the immobilization of natural polymers such as silica, resins, silica composites, and magnetic materials among others. Magnetic nanoparticles based on metals such as Cu, Co, Fe, and Ni provide a potent solid support system to immobilize proteins^{6–10}, among them, magnetite nanoparticles (Fe_3O_4) have remarkable properties such as superparamagnetism, low toxicity, high specific surface area, biocompatibility and easy separation which makes them more interesting for researchers.

One of the most commonly used techniques for the immobilization of proteins is cross-linking. For collagen materials, many crosslinkers such as glutaraldehyde, isocyanates, glyoxal, and carbodiimides, were used¹¹.

Natural polymers such as polysaccharides (cellulose, chitosan, chitin, alginate, carrageenan, lignin, fucoidan, etc.) and proteins have been used as catalysts in chemical transformations^{12–18}. Coating magnetic particles with natural polymers allows them to use their functional groups for promoting chemical reactions and also easy separation^{19,20}.

Based on our interest for turning agricultural and marine waste into value added materials^{21–23}, we have used Isinglass (IG), a natural polymer derived from swim bladder of fish with high content of collagen protein, for encapsulating $\text{Fe}_3\text{O}_4@\text{SiO}_2$ nanoparticles using epichlorohydrin (ECH) as crosslinking agent. The prepared hybrid material named $\text{Fe}_3\text{O}_4@\text{SiO}_2/\text{ECH}/\text{IG}$ was applied as bifunctional heterogeneous catalyst in the synthesis of spirooxindole derivatives. Such hybrid material based on natural polymer IG with both acidic and basic groups has been shown to be a very effective catalyst in a variety of chemical transformation, including the synthesis of,

Heterocyclic Chemistry Research Laboratory, Department of Chemistry, Iran University of Science and Technology, 16846-13114 Tehran, Iran. ✉email: shjavan@iust.ac.ir

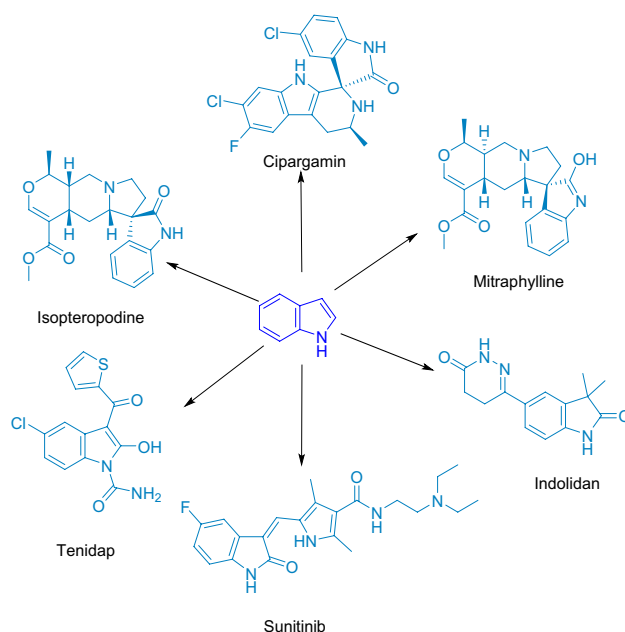


Figure 1. Some biologically active oxindoles and spirooxindoles.

triazoles²⁴, 4*H*-pyran derivatives²⁵, and Suzuki coupling²⁶. IG contains many amino acids whose properties and catalytic performances have been demonstrated for many years^{27,28}.

Defined as processes allowing at least three reagents to react in a single pot, all of which participate in the structure of the final product, multicomponent reactions make it possible to synthesize highly functionalized compounds. In addition, multicomponent reactions offer rapid access to a wide variety of potential active ingredients. In the same way that a 4-digit code offers 10,000 possibilities, the possible variations for each reagent give access to an impressive number of related compounds. Very useful in combinatorial chemistry, MCRs make it possible to constitute chemical libraries for high throughput screening in the pharmaceutical industry. Several evocative tags are commonly involved in MCRs such as the atomic economy, easy to implement, using very mild reaction conditions, and without recourse to toxic metals, these reactions represent a definite step forward to ideal synthesis^{29,30}.

Heterocyclic compounds represent more than 90% of the active ingredients possessing a wide range of applications in pharmaceutical industry, veterinary medicine and phytochemistry³¹. Indoles, oxindoles, and spirooxindoles are important heterocyclic compounds, and ubiquitous motifs in naturally and unnaturally occurring biologically active pharmaceutical ingredients³⁰. Some biologically active indoles, oxindoles and spirooxindoles are presented in Fig. 1.

So far, various methods and catalysts have been used for the synthesis of these compounds, including the reaction between isatin, malononitrile and dimedone with different catalysts such as α -amylase³², $\text{CoFe}_2\text{O}_4@ \text{SiO}_2@ \text{SO}_3\text{H}$ ³³, $\text{MgO}@ \text{PMO-IL}$ ³⁴, magnetic sulfonated chitosan³⁵, magnetic poly ethyleneimine³⁶, etc.

Here, we have developed a new collagen-coated superparamagnetic iron oxide nanoparticle as a sustainable bio-based catalyst for the direct synthesis of spirooxindole (Fig. 2).

Results and discussion

Synthesis pathway of $\text{Fe}_3\text{O}_4@ \text{SiO}_2/ \text{ECH}/ \text{IG}$ is illustrated in Fig. 3. Fe_3O_4 NPs were prepared through a co-precipitation method by dissolving divalent and trivalent iron salts into distilled water, followed by precipitation with NH_4OH . Afterward, TEOS was hydrolyzed to form silica oligomers, which were coated on the surface of Fe_3O_4 nanoparticles to obtain $\text{Fe}_3\text{O}_4@ \text{SiO}_2$ nanoparticles. Subsequently, ECH was cross-linked on the surface of $\text{Fe}_3\text{O}_4/ \text{SiO}_2$. $\text{Fe}_3\text{O}_4@ \text{SiO}_2/ \text{ECH}/ \text{IG}$ was obtained by nucleophilic addition of IG to as-prepared magnetic nanoparticles.

Characterization of the $\text{Fe}_3\text{O}_4@ \text{SiO}_2/ \text{ECH}/ \text{IG}$. The structure, morphology and magnetic properties of the prepared nanocatalyst were accurately characterized by different analytical techniques. The FT-IR spectra of the $\text{Fe}_3\text{O}_4@ \text{SiO}_2/ \text{ECH}/ \text{IG}$, $\text{Fe}_3\text{O}_4@ \text{SiO}_2$, and Fe_3O_4 are compared in Fig. S1 (see supporting information). The FTIR spectrum of Fe_3O_4 indicates the characteristic band of Fe–O at 596 cm^{-1} ³⁷.

The sharp bands at 1072 cm^{-1} and 816 cm^{-1} were assigned to the asymmetric and symmetric linear stretching vibrations of Si–O–Si bonding respectively. The bending vibration absorption peak of Si–O–Si was also perceived at 464 cm^{-1} ³⁸. The absorption peak at 3426 cm^{-1} which was assigned to the O–H stretching vibrations was shifted from 3426 to 3276 cm^{-1} in $\text{Fe}_3\text{O}_4@ \text{SiO}_2/ \text{ECH}/ \text{IG}$ with a net diminution of intensity indicating the involvement of isinglass in the synthesis of final composite. The characteristic bands appeared at 1400 , 1385 and 1220 cm^{-1}



Figure 2. Collagen-coated superparamagnetic iron oxide nanoparticles as a sustainable bio-based catalyst for the direct synthesis of spirooxindole (software used: ChemDraw Ultra 12.0 and Paint 3D).

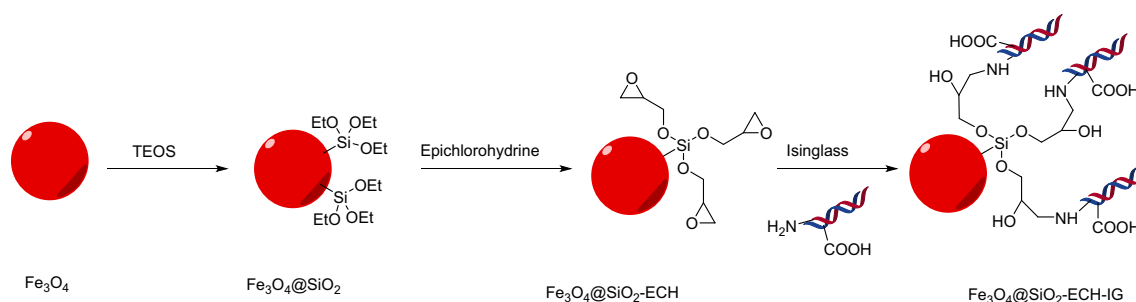


Figure 3. Schematic representation of the catalyst synthesis procedures.

were attributed to C–O (carboxyl), C–OH (secondary) and C–O groups. Finally, this FT-IR spectrum can be clearly shown that the $\text{Fe}_3\text{O}_4@/\text{SiO}_2/\text{ECH}/\text{IG}$ was successfully prepared.

The morphology and the structure of the $\text{Fe}_3\text{O}_4@/\text{SiO}_2/\text{ECH}/\text{IG}$ was characterized by SEM and TEM analysis (Fig. 4a,b,c). The average particle size was estimated to be 58 nm. Moreover, the well-ordered structure of the catalyst and its almost uniform distribution are clearly observable (Fig. 4a). The core–shell structure of the magnetic particles was proofed with the black centres and the brightest areas as Fe_3O_4 cores and SiO_2 shells respectively. These images also approve that the particles are nanometric in size (Fig. 4b). Moreover, the TEM images of the catalyst after the recycling process show that the structure of the nanocatalyst didn't change during the reaction (Fig. 4c), which provides clear evidence of the stability of the prepared catalyst.

Furthermore, the presence of carbon, oxygen, nitrogen, iron and Si elements (ratios of 23.43: 61.92: 6.77: 6.15: 1.69 wt%, respectively) was confirmed by EDX analysis shown in Fig. 5a and b. It confirms that the incorporation of expected elements into the structure of the prepared catalyst was achieved successfully.

The magnetic features of Fe_3O_4 , $\text{Fe}_3\text{O}_4@/\text{SiO}_2$ and $\text{Fe}_3\text{O}_4@/\text{SiO}_2/\text{ECH}/\text{IG}$ were investigated using VSM analysis and the magnetization cycles of the samples are plotted in Fig. 6. As it can be noticed, the particles have zero remanent magnetization so the particles display superparamagnetic behavior. The lack of net magnetization in the absence of an external field allows superparamagnetic nanoparticles to avoid magnetic aggregation³⁹. Magnetic hysteresis loop measurements indicated that the maximum saturation magnetization value of $\text{Fe}_3\text{O}_4@/\text{SiO}_2/\text{ECH}/\text{IG}$ ($17.162 \text{ emus g}^{-1}$) was less than Fe_3O_4 (63.9 emus g^{-1}) which proved the incorporation of IG on the surface of Fe_3O_4 (Fig. 5)²⁵.

In Fig. 7, the XRD pattern of $\text{Fe}_3\text{O}_4@/\text{SiO}_2/\text{ECH}/\text{IG}$ shows the six characteristic diffraction peaks at 2θ 30.064°, 35.452°, 43.038°, 53.547°, 57.168°, and 62.728° corresponding to the (220), (311), (400), (422), (511), and (440) reflection crystal plans of Fe_3O_4 respectively (JCPDS card no. 00-001-1111, 00-002-0459). The broad diffraction peak at 2θ value 10–20° was attributed to the amorphous structure of isinglass²⁵. Another broad diffraction peak around 25–35° indicated the formation of an amorphous SiO_2 shell around Fe_3O_4 (JCPDS card no.00-002-0278). (The reference card numbers were collected from the X'pert HighScore Plus version 1.0d software developed by the PANalytical B.V.).

The specific surface area, pore volume and size analysis were determined by BET methods. According to the BET analysis results shown in Fig. S2 (see supporting information), the adsorption–desorption isotherms display

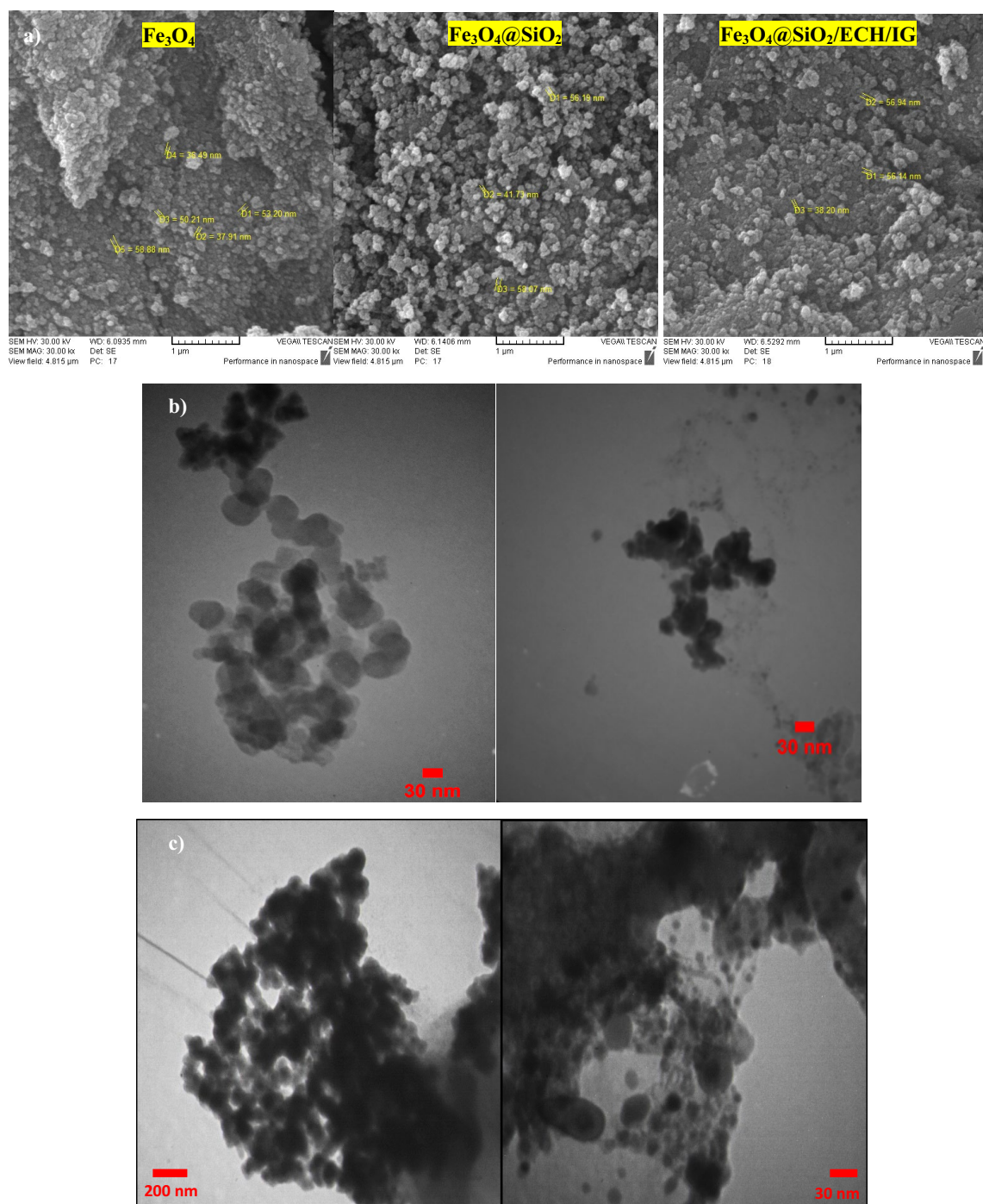


Figure 4. (a) SEM images of Fe_3O_4 , $\text{Fe}_3\text{O}_4@\text{SiO}_2$ and $\text{Fe}_3\text{O}_4@\text{SiO}_2/\text{ECH}/\text{IG}$ and (b) TEM images of $\text{Fe}_3\text{O}_4@\text{SiO}_2/\text{ECH}/\text{IG}$ before reaction and (c) TEM images of $\text{Fe}_3\text{O}_4@\text{SiO}_2/\text{ECH}/\text{IG}$ after recycling.

a type IV isotherm with an H_3 hysteresis loop. The BET surface area is $8.4324 \text{ m}^2/\text{g}$ and the adsorption average pore diameter (4 V/A by BET) is 24.49352 nm . The single-point adsorption total pore volume is $0.051635 \text{ cm}^3/\text{g}$ (Table S4, see supporting information).

To investigate the thermal stability of the $\text{Fe}_3\text{O}_4@\text{SiO}_2/\text{ECH}/\text{IG}$, its thermogravimetric analysis (TGA) was carried out under Ar atmosphere at a temperature varying from 50 to 800 °C. The total weight loss of the nanocatalyst was around 50% (Fig. S3 (see supporting information)). The first weight loss at around 100 °C is attributed to the physically adsorbed water or residual organic solvents in the prepared nanocatalyst. The weight loss at ~ 250 °C continued to ~ 400 °C is related to decomposition of collagen peptide and grafted molecules onto silica surface. The last weight loss from 400 to 800 °C can be ascribed to the combustion of residual coating agents.

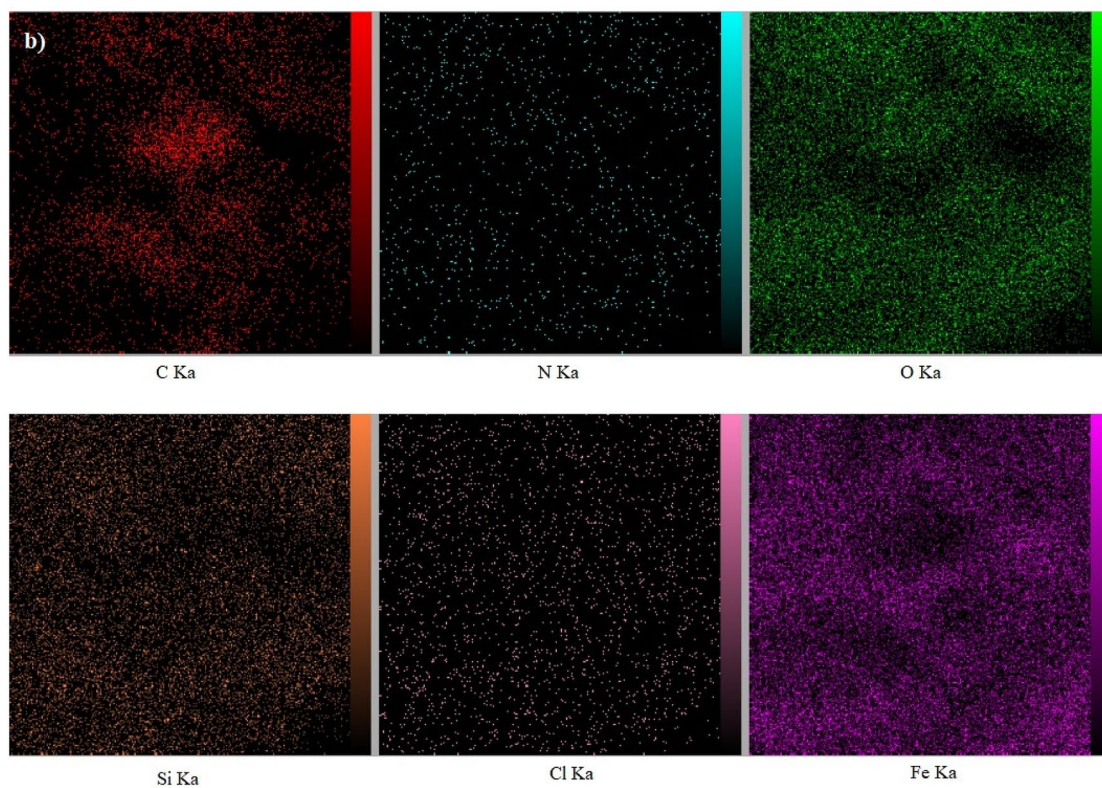
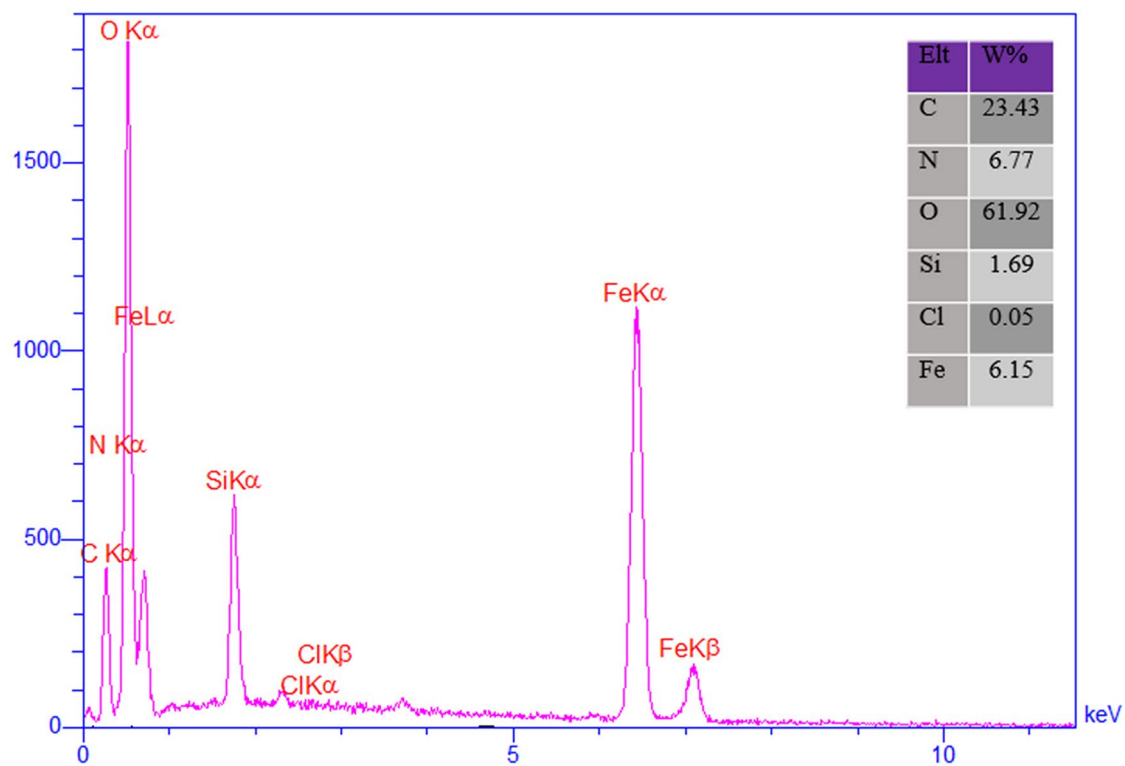


Figure 5. (a) Energy dispersive X-ray analysis (EDX) of $\text{Fe}_3\text{O}_4@/\text{SiO}_2/\text{ECH}/\text{IG}$ and (b) elemental mapping of C (red); N (blue), O (green), Fe (violet), Si (orange) and Cl (pink) atoms for $\text{Fe}_3\text{O}_4@/\text{SiO}_2/\text{ECH}/\text{IG}$.

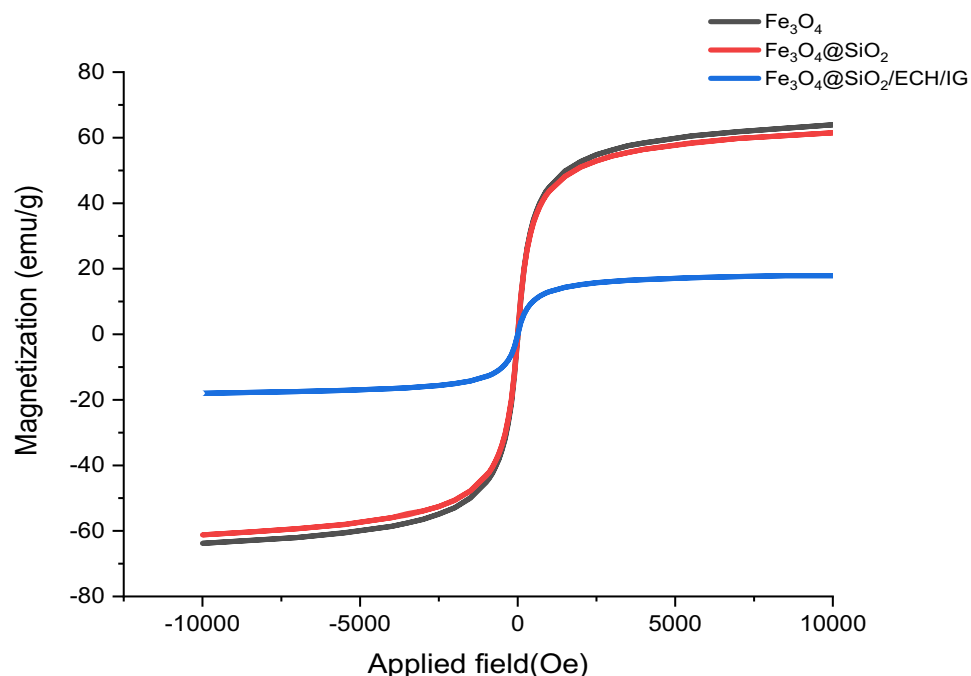


Figure 6. VSM analysis of the prepared $\text{Fe}_3\text{O}_4@SiO_2/ECH/IG$.

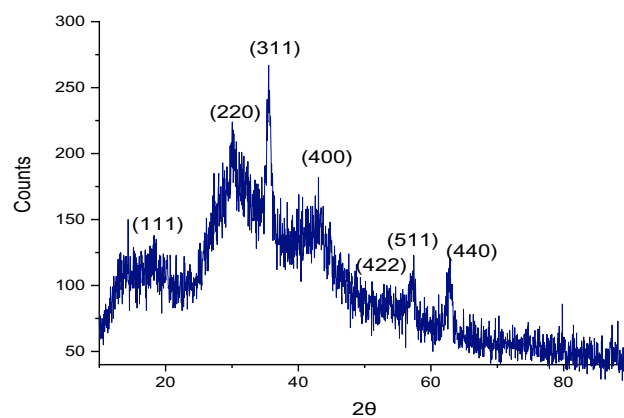


Figure 7. XRD pattern of $\text{Fe}_3\text{O}_4@SiO_2/ECH/IG$.

Investigation the catalytic activities of $\text{Fe}_3\text{O}_4@SiO_2/ECH/IG$ for the synthesis of spirooxindole derivatives 4a-t. The catalytic behavior of $\text{Fe}_3\text{O}_4@SiO_2/ECH/IG$ was investigated for the synthesis of spirooxindole derivatives via a three- component reaction between CH-acids, malononitrile, and isatin derivatives under different conditions. To find the optimal reaction conditions, various factors such as catalyst loading, solvent, time and reaction temperature were scrutinized in a model reaction including dimedone (**1a**), malononitrile (**2a**), and isatin (**3a**) to estimate the proper catalytic loading and time (Fig. 8). Amid different solvents, the mixture of EtOH/ H_2O (1:1) was completed in a shorter time and gave a better yield (Table S1).

For further optimization, the effect of temperature, type of catalyst, and the amount of catalyst were also investigated and tabulated in Table S2 and S3 (See supporting information). The results revealed the high performance of $\text{Fe}_3\text{O}_4@SiO_2/ECH/IG$ due to synergistic effects and improved number of active sites on surface. The highest conversion of 94% was reached for 10 mg catalyst loading at 60 °C. Obviously, the increase in catalyst loading was not favorable. On the other hand, with an amount of catalyst of 10 mg, lowering the temperature leads to a decrease in the reaction yield.

To generalize the optimum conditions, different spirooxindole derivatives from 4a-t were prepared through a one pot reaction of isatin derivatives 1, malononitrile 2 and 1,3 dicarbonyl derivatives **3a–3e** in the presence of $\text{Fe}_3\text{O}_4@SiO_2/ECH/IG$ (Fig. 7). The results are summarized in Table 1. As expected, the presence of electron-withdrawing groups on isatin can enhance the rate and yield of the reaction. The best result in the shortest time

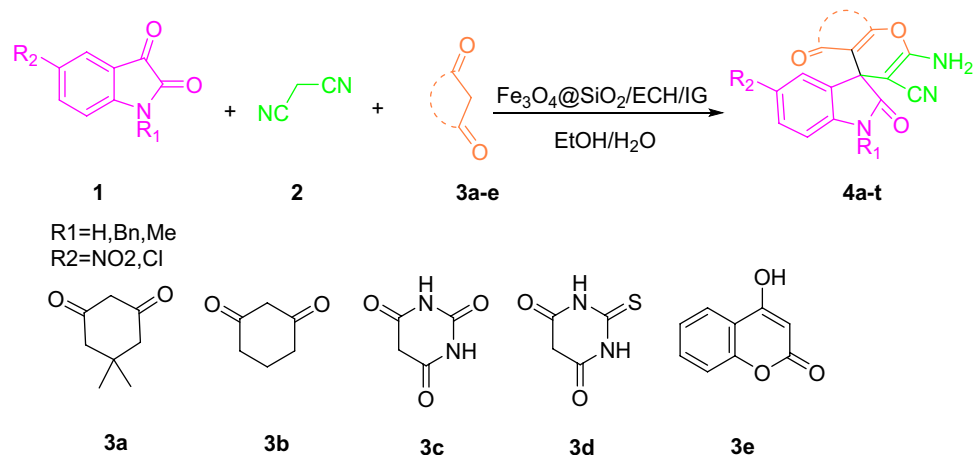


Figure 8. Schematic representation of the $\text{Fe}_3\text{O}_4@\text{SiO}_2/\text{ECH/IG}$ and its catalytic activity in the one-pot synthesis of spirooxindole derivatives (4a-t) through multicomponent reaction (MCR) strategy.

Entry	R ₁	R ₂	1,3-dicarbonyl compound	Time (min)	Yield (%)	m.p. °C (reported)	Product
1	H	H	3a	10	94	301–303 (302–306) ⁴⁰	4a
2	H	H	3b	10	88	282–284 (278–280) ⁴¹	4b
3	H	H	3c	20	81	267–268 (268–270) ⁴¹	4c
4	H	H	3d	15	85	230–232 (240–241) ⁴⁰²	4d
5	H	H	3e	25	80	301–303 (290–292) ²¹	4e
6	H	NO ₂	3a	10	89	> 300 (302–304) ⁴¹³	4f.
7	H	NO ₂	3b	5	85	> 300 (306–307) ⁴²⁴	4g
8	H	NO ₂	3c	5	93	286–288 (288–289) ⁴³⁵	4h
9	H	NO ₂	3d	10	98	240–242 (253–255) ⁴⁴⁶	4i
10	H	NO ₂	3e	30	82	297–299 (294–296) ⁴⁵⁷	4j
11	H	Cl	3c	20	70	234–236 (240–242) ⁴⁶	4k
12	H	Cl	3e	30	79	> 300 (300–302) ⁴⁶	4l
13	Bn	H	3a	10	86	284–286 (281–282) ⁴⁷	4m
14	Bn	H	3b	5	92	282–284 (282–284) ⁴⁸	4n
15	Bn	H	3e	30	88	273–275 (280–282) ⁴⁹	4o
16	Me	H	3a	10	80	260–262 (255–258) ⁵⁰	4p
17	Me	H	3b	10	83	244–246 (243–245) ⁵¹	4q
18	Me	H	3c	35	94	279–281 (285–286) ⁵²	4r
19	Me	H	3d	15	92	274–276 (280–282) ⁵³	4s
20	Me	H	3e	30	83	281–283 (283–285) ⁵⁴	4t

Table 1. Synthesis of spirooxindole derivatives in the presence of $\text{Fe}_3\text{O}_4@\text{SiO}_2/\text{ECH/IG}$. *Reaction condition: Isatin 1 (1 mmol), 2 (1 mmol), 1,3-dicarbonyl 3 (1 mmol), 10 mg catalyst, and 3 ml solvent at 60 °C.

was related to the 5-nitro isatin derivative. Contrariwise, the isatin with an electron-donating group provided product with a lower yield.

The proposed mechanism of the model reaction for spirooxindole derivative synthesis is mentioned in Fig. 9. In the first step the bifunctional catalyst activated the carbonyl group of isatin by protonation. On the other hand, the amine group of catalyst take the acidic hydrogen of malononitrile. The 1,3 dicarbonyl derivatives was activated and became to enol form through the interaction with functional group of isinglass. The reaction of the first intermediate with activated enol form of dicarbonyl derivatives gives the intermediate (II). Cyclisation, dehydration and tautomerization of imine formed the desire product.

Catalyst recyclability. The easy separation of $\text{Fe}_3\text{O}_4@\text{SiO}_2/\text{ECH/IG}$ heterogenous catalyst was mentioned further. In this regard, the recyclability of the nanocatalyst in the model reaction was investigated. At the end of the reaction, $\text{Fe}_3\text{O}_4@\text{SiO}_2/\text{ECH/IG}$ was collected by an external magnetic field and washed with ethanol and water. The dried magnetic nanocatalyst was successively used for four times in the model reaction with a yield as 89%. According to the results displayed in Fig. S4 (see supporting information), there is no significant reduction in the catalytic efficiency of $\text{Fe}_3\text{O}_4@\text{SiO}_2/\text{ECH/IG}$. FTIR spectra of the recycled catalyst were recorded after

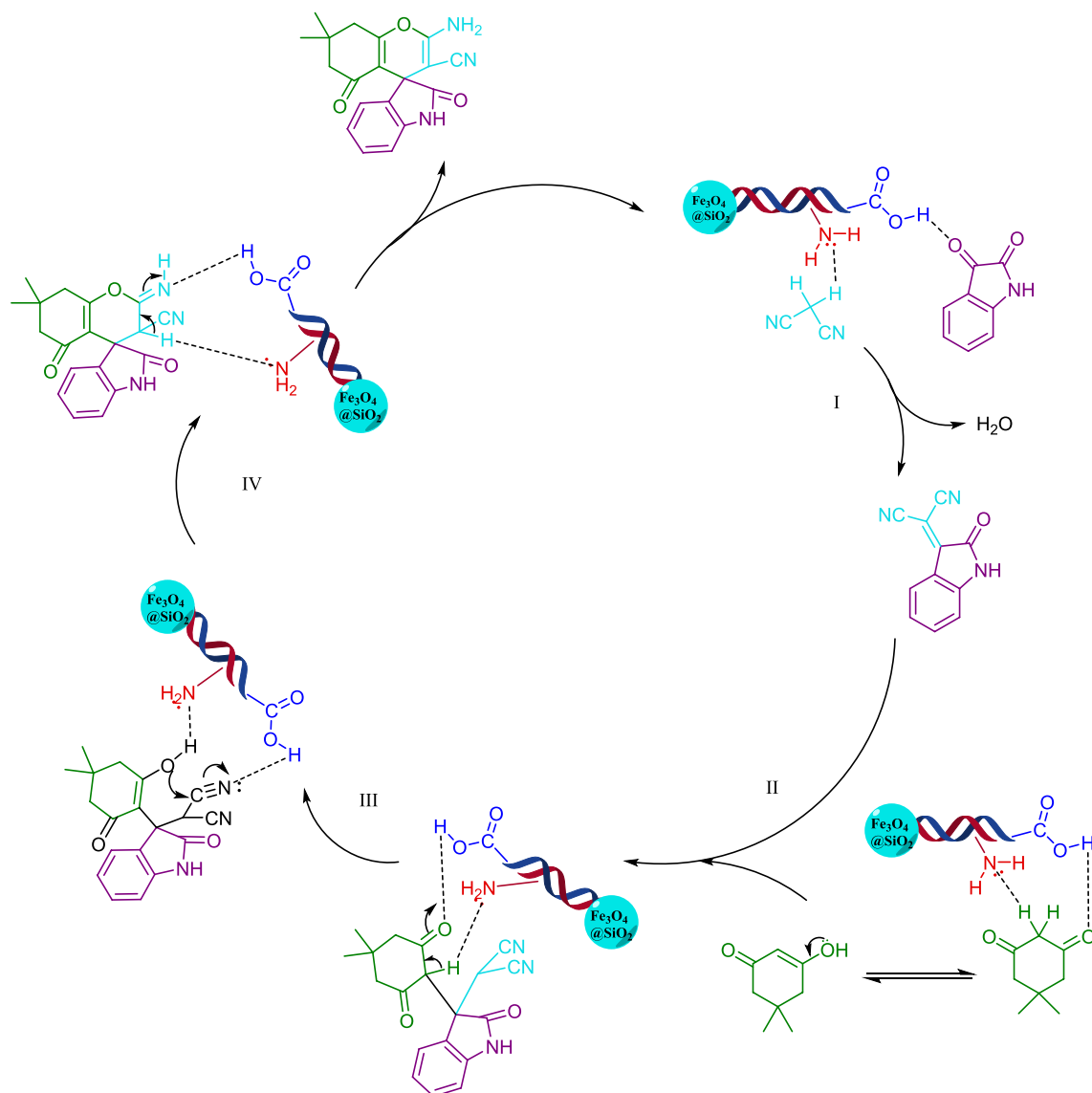


Figure 9. Proposed catalytic mechanism of $\text{Fe}_3\text{O}_4@/\text{SiO}_2/\text{ECH}/\text{IG}$.

Entry	Catalyst	Conditions	Time(min)	Yield (%)	References
1	[Bmim]OH	Solvent free/R.T	600	98	55
2	Tris-hydroxymethyl aminomethane	Ethanol/R.T	240	94	56
3	Trisodium citrate dihydrate	EtOH:Water/R.T	120	96	57
4	g- $\text{C}_3\text{N}_4/\text{SO}_3\text{H}$	EtOH:Water/reflux	40	95	58
5	$\text{Fe}_3\text{O}_4@/\text{SiO}_2/\text{ECH}/\text{IG}$	EtOH:Water/60 °C	10	94	This work

Table 2. Comparison of the present catalyst for the synthesis of spirooxindole derivatives with reported studies.

multiple cycles and compared with the fresh catalyst (Fig. S1). It is clear that the used catalyst has not endure any structural changes.

In order to demonstrate the efficacy of the prepared $\text{Fe}_3\text{O}_4@/\text{SiO}_2/\text{ECH}/\text{IG}$ catalyst, the catalytic activity in the preparation of spirooxindole derivatives was compared with the previous reports. The present catalyst has several advantages in terms of reaction time, solvent, and yield over the reported studies which are tabulated in Table 2.

Experimental section. *Reagents and apparatus.* All reagents and materials were purchased from commercial sources and used without purification. All of them were analytical grade. The commercially swim blad-

ders were purchased from grocery store. The known products were identified by comparison of their melting points. Melting points were determined in open capillaries using an Electrothermal 9100 instrument. Infrared (IR) spectra were acquired on a Shimadzu FT-IR-8400S spectrometer with spectroscopic grade KBr. The ^1H NMR (500 MHz) were obtained on a Bruker Avance DPX-300 instrument. The spectra were obtained in DMSO- d_6 relative to TMS as internal standard. Scanning electron microscopy (SEM) was recorded on a VEG2/TESCAN 30kv with gold coating, and energy dispersive X-ray spectroscopy (EDX) was recorded on a VEG//TESCAN-XMU.

General procedure for the preparation of the $\text{Fe}_3\text{O}_4@\text{SiO}_2$ NPs. The superparamagnetic iron oxide nanoparticles (SPIONs) were synthesized using a co-precipitation method described before^{59,60}. Typically, $\text{FeCl}_3 \cdot 6\text{H}_2\text{O}$ (1.215 g) and $\text{FeCl}_2 \cdot 4\text{H}_2\text{O}$ (0.637 g) ($\text{Fe}^{2+}/\text{Fe}^{3+} = 1:2$) were dissolved in deionized water (20 mL) under an inert atmosphere to get a homogenous solution. Chemical precipitation was carried out by the slow addition of NaOH solution (25%), stirring vigorously at 80 °C for 60 min, until the pH = 10 was attained. The obtained magnetic particles were separated by an external magnetic field, washed three times with deionized water and ethanol (25 mL), and dried in a 65 °C oven for 24 h. After that 1 g of the prepared Fe_3O_4 was dispersed in deionized water (50 mL) and stirred for 30 min. Next, a mixture of ammonia (5 ml) and ethanol (50 ml) was added to the flask followed by adding 1.5 ml TEOS. The mixture was stirred for 24 h in room temperature. The prepared $\text{Fe}_3\text{O}_4@\text{SiO}_2$ was magnetically separated, washed sequentially with water and ethanol and dried in a vacuum oven at 50 °C⁶¹.

General procedure for the preparation of $\text{Fe}_3\text{O}_4@\text{SiO}_2/\text{ECH}$. To prepare $\text{Fe}_3\text{O}_4@\text{SiO}_2/\text{ECH}$ nanoparticles, 1 g of the obtained $\text{Fe}_3\text{O}_4@\text{SiO}_2$ was poured into a round bottom flask containing 3 ml ethanol. Then, ECH (1 ml) was slowly added and the mixture was stirred for 5 h at 60 °C. The resulting precipitate was then magnetically separated, washed with water and ethanol to remove unreacted reagents, and dried in a vacuum oven at 50 °C⁶².

General procedure for the preparation of $\text{Fe}_3\text{O}_4@\text{SiO}_2/\text{ECH}/\text{IG}$. Initially the isinglass was milled to obtain a white powder. 0.1 g of the dried $\text{Fe}_3\text{O}_4@\text{SiO}_2$ was dissolved in 20 ml ethanol and mixed with 0.2 g of isinglass. The mixture was sonicated for 30 min and then stirred at room temperature for 1 h. finally the obtained precipitate was magnetically separated, washed with water and ethanol and dried at 50 °C.

General experimental procedure for the synthesis of benzimidazoles derivatives catalysed by $\text{Fe}_3\text{O}_4@\text{SiO}_2/\text{ECH}/\text{IG}$. A mixture of isatin (1 mmol), malononitrile (1 mmol), various 1,3 dicarbonyls (1 mmol), and $\text{Fe}_3\text{O}_4@\text{SiO}_2/\text{ECH}/\text{IG}$ (0.02 g) in EtOH/water (1:1) had been stirred for an appropriate period of time. After completion of the reaction as indicated by TLC, the reaction mixture had been dissolved in hot ethanol and the catalyst was recovered by an external magnet, washed, dried and then reused in successive reaction. The reaction mixture had been recrystallized with ethanol to afford pure desired substituted benzimidazoles⁶³.

Conclusions

In summary, we devised a novel collagen-coated superparamagnetic organic–inorganic hybrid catalyst, $\text{Fe}_3\text{O}_4@\text{SiO}_2/\text{ECH}/\text{IG}$, which exhibited radically enhanced catalytic activity in the synthesis of a wide range of substituted spirooxindole derivatives through a one pot atom economical condensation of isatin, dimedone, and malononitrile under mild conditions. This bifunctional heterogeneous catalyst efficiency is achieved in several aspects, such as high product yields under mild conditions, stability, recyclability, and high reaction rate. Furthermore, the easy separation and removal from the reaction environment makes this catalyst a good choice for use in drug synthesis applications. These results affirmed that the novel $\text{Fe}_3\text{O}_4@\text{SiO}_2/\text{ECH}/\text{IG}$ can be considered as a versatile catalyst for promoting chemical reactions.

Received: 9 May 2021; Accepted: 24 February 2022

Published online: 12 April 2022

References

- Zhao, Z.-S., Zhang, Y., Fang, T., Han, Z.-B. & Liang, F.-S. Chitosan-coated metal–organic-framework nanoparticles as catalysts for tandem deacetalization-knoevenagel condensation reactions. *ACS Appl. Nano Mater.* **3**, 6316–6320 (2020).
- Veisi, H., Ozturk, T., Karmakar, B., Tamoradi, T. & Hemmati, S. In situ decorated Pd NPs on chitosan-encapsulated $\text{Fe}_3\text{O}_4/\text{SiO}_2\text{-NH}_2$ as magnetic catalyst in Suzuki-Miyaura coupling and 4-nitrophenol reduction. *Carbohydr. Polym.* **235**, 115966 (2020).
- Amirnejat, S., Nosrati, A., Javanshir, S. & Naimi-Jamal, M. R. Superparamagnetic alginate-based nanocomposite modified by L-arginine: An eco-friendly bifunctional catalysts and an efficient antibacterial agent. *Int. J. Biol. Macromol.* **152**, 834–845 (2020).
- Ali, F., Khan, S. B., Shaheen, N. & Zhu, Y. Z. Eggshell membranes coated chitosan decorated with metal nanoparticles for the catalytic reduction of organic contaminates. *Carbohydr. Polym.* **2**, 117681 (2021).
- Zhou, Y., Shen, J., Bai, Y., Li, T. & Xue, G. Enhanced degradation of Acid Red 73 by using cellulose-based hydrogel coated Fe_3O_4 nanocomposite as a Fenton-like catalyst. *Int. J. Biol. Macromol.* **152**, 242–249 (2020).
- Ohata, J., Martin, S. C. & Ball, Z. T. Metal-mediated functionalization of natural peptides and proteins: Panning for bioconjugation gold. *Angew. Chem. Int. Ed.* **58**, 6176–6199 (2019).
- Li, X. *et al.* Highly active enzyme–metal nanohybrids synthesized in protein–polymer conjugates. *Nat. Catal.* **2**, 718–725 (2019).
- Patel, S. K. *et al.* Synthesis of cross-linked protein-metal hybrid nanoflowers and its application in repeated batch decolorization of synthetic dyes. *J. Hazard. Mater.* **347**, 442–450 (2018).
- Patel, S. K., Otari, S. V., Kang, Y. C. & Lee, J.-K. Protein–inorganic hybrid system for efficient his-tagged enzymes immobilization and its application in L-xylulose production. *RSC Adv.* **7**, 3488–3494 (2017).

10. Li, C., Jiang, S., Zhao, X. & Liang, H. Co-immobilization of enzymes and magnetic nanoparticles by metal-nucleotide hydrogel-nanofibers for improving stability and recycling. *Molecules* **22**, 179 (2017).
11. Mylkie, K., Nowak, P., Rybczynski, P. & Ziegler-Borowska, M. Polymer-coated magnetite nanoparticles for protein immobilization. *Materials* **14**, 248 (2021).
12. Saneinezhad, S., Mohammadi, L., Zadsirjan, V., Bamoharram, F. F. & Heravi, M. M. Silver nanoparticles-decorated Preyssler functionalized cellulose biocomposite as a novel and efficient catalyst for the synthesis of 2-amino-4-H-pyrans and spirochromenes. *Sci. Rep.* **10**, 1–26 (2020).
13. Dolatkah, Z., Javanshir, S., Bazgir, A. & Hemmati, B. Palladium on magnetic Irish moss: A new nano-biocatalyst for suzuki type cross-coupling reactions. *Appl. Organomet. Chem.* **33**, e4859 (2019).
14. Liu, Y., Xu, H., Yu, H., Yang, H. & Chen, T. Synthesis of lignin-derived nitrogen-doped carbon as a novel catalyst for 4-NP reduction evaluation. *Sci. Rep.* **10**, 1–14 (2020).
15. Tan, J. M., Bullo, S., Fakurazi, S. & Hussein, M. Z. Preparation, characterisation and biological evaluation of biopolymer-coated multi-walled carbon nanotubes for sustained-delivery of silibinin. *Sci. Rep.* **10**, 1–15 (2020).
16. Çalıskan, M. & Baran, T. Decorated palladium nanoparticles on chitosan/ δ -FeOOH microspheres: A highly active and recyclable catalyst for Suzuki coupling reaction and cyanation of aryl halides. *Int. J. Biol. Macromol.* **2**, 190 (2021).
17. Nasrollahzadeh, M., Shafei, N., Nezafat, Z., Bidgoli, N. S. S. & Soleimani, F. Recent progresses in the application of cellulose, starch, alginate, gum, pectin, chitin and chitosan based (nano) catalysts in sustainable and selective oxidation reactions: A review. *Carbohydr. Polym.* **6**, 116353 (2020).
18. Banazadeh, M., Amirnejat, S. & Javanshir, S. Synthesis, characterization, and catalytic properties of magnetic Fe₃O₄@FU: A heterogeneous nanostructured mesoporous bio-based catalyst for the synthesis of imidazole derivatives. *Front. Chem.* **8**, 1089 (2020).
19. Veisi, H., Mohammadi, L., Hemmati, S., Tamoradi, T. & Mohammadi, P. In situ immobilized silver nanoparticles on rubia tinctum extract-coated ultrasmall iron oxide nanoparticles: An efficient nanocatalyst with magnetic recyclability for synthesis of propargylamines by A₃ coupling reaction. *ACS Omega* **4**, 13991–14003 (2019).
20. Rajabi-Moghaddam, H., Naimi-Jamal, M. & Tajbaksh, M. Fabrication of copper (II)-coated magnetic core-shell nanoparticles Fe₃O₄@SiO₂-2-aminobenzohydrazide and investigation of its catalytic application in the synthesis of 1, 2, 3-triazole compounds. *Sci. Rep.* **11**, 1–14 (2021).
21. Javanshir, S., Pourshiri, N. S., Dolatkah, Z. & Farhadnia, M. Caspian Isinglass, a versatile and sustainable biocatalyst for domino synthesis of spirooxindoles and spiroacenaphthylenes in water. *Monatshefte für Chemie-Chemical Monthly* **148**, 703–710 (2017).
22. Dekamin, M. G. *et al.* Sodium alginate: An efficient biopolymeric catalyst for green synthesis of 2-amino-4H-pyran derivatives. *Int. J. Biol. Macromol.* **87**, 172–179 (2016).
23. Hemmati, B., Javanshir, S. & Dolatkah, Z. Hybrid magnetic Irish moss/Fe₃O₄ as a nano-biocatalyst for synthesis of imidazopyrimidine derivatives. *RSC Adv.* **6**, 50431–50436 (2016).
24. Dolatkah, Z., Javanshir, S., Bazgir, A. & Mohammadkhani, A. Magnetic isinglass a nano-bio support for copper immobilization: Cu-IG@Fe₃O₄ a heterogeneous catalyst for triazoles synthesis. *ChemistrySelect* **3**, 5486–5493 (2018).
25. Pourian, E., Javanshir, S., Dolatkah, Z., Molaei, S. & Maleki, A. Ultrasonic-assisted preparation, characterization, and use of novel biocompatible core/shell Fe₃O₄@GA@isinglass in the synthesis of 1, 4-dihydropyridine and 4 H-pyran derivatives. *ACS Omega* **3**, 5012–5020 (2018).
26. Dolatkah, Z., Javanshir, S. & Bazgir, A. Isinglass–palladium as collagen peptide–metal complex: A highly efficient heterogeneous biocatalyst for Suzuki cross-coupling reaction in water. *J. Iran. Chem. Soc.* **16**, 1473–1481 (2019).
27. Burate, P. A., Javle, B. R., Desale, P. H. & Kinage, A. K. Amino acid amide based ionic liquid as an efficient organo-catalyst for solvent-free Knoevenagel condensation at room temperature. *Catal. Lett.* **149**, 2368–2375 (2019).
28. Wang, J. *et al.* Efficient conversion of N-acetyl-d-glucosamine into nitrogen-containing compound 3-acetamido-5-acetylfuran using amino acid ionic liquid as the recyclable catalyst. *Sci. Total Environ.* **710**, 136293 (2020).
29. Demurtas, M. *et al.* Indole derivatives as multifunctional drugs: Synthesis and evaluation of antioxidant, photoprotective and antiproliferative activity of indole hydrazones. *Bioorg. Chem.* **85**, 568–576 (2019).
30. Nájera, C. & Sansano, J. M. Synthesis of pyrrolizidines and indolizidines by multicomponent 1, 3-dipolar cycloaddition of azomethine ylides. *Pure Appl. Chem.* **91**, 575–596 (2019).
31. Karimi, A. R. & Sedaghatpour, F. Novel mono- and bis (spiro-2-amino-4H-pyrans): Alum-catalyzed reaction of 4-hydroxycoumarin and malononitrile with isatins, quinones, or ninhydrin. *Synthesis* **2010**, 1731–1735 (2010).
32. He, T., Zeng, Q.-Q., Yang, D.-C., He, Y.-H. & Guan, Z. Biocatalytic one-pot three-component synthesis of 3, 3'-disubstituted oxindoles and spirooxindole pyrans using α -amylase from hog pancreas. *RSC Adv.* **5**, 37843–37852 (2015).
33. Zamani-Ranjbar-Garmroodi, B., Nasseri, M. A., Allahresani, A. & Hemmat, K. Application of immobilized sulfonic acid on the cobalt ferrite magnetic nanocatalyst (CoFe₂O₄@SiO₂@SO₃H) in the synthesis of spirooxindoles. *Res. Chem. Intermed.* **45**, 5665–5680 (2019).
34. Baharfar, R., Zareyee, D. & Allahgholipour, S. L. Synthesis and characterization of MgO nanoparticles supported on ionic liquid-based periodic mesoporous organosilica (MgO@PMO-IL) as a highly efficient and reusable nanocatalyst for the synthesis of novel spirooxindole-furan derivatives. *Appl. Organomet. Chem.* **33**, e4805 (2019).
35. Naeimi, H. & Lahouti, S. Sulfonated chitosan encapsulated magnetically Fe₃O₄ nanoparticles as effective and reusable catalyst for ultrasound-promoted rapid, three-component synthesis of spiro-4H-pyrans. *J. Iran. Chem. Soc.* **15**, 2017–2031 (2018).
36. Khoobi, M. *et al.* Polyethyleneimine-modified superparamagnetic Fe₃O₄ nanoparticles: An efficient, reusable and water tolerance nanocatalyst. *J. Magn. Magn. Mater.* **375**, 217–226 (2015).
37. Sun, J. *et al.* Synthesis and characterization of biocompatible Fe₃O₄ nanoparticles. *J. Biomed. Mater. Res. Part A* **80**, 333–341 (2007).
38. Cai, W. *et al.* Modified green synthesis of Fe₃O₄@SiO₂ nanoparticles for pH responsive drug release. *Mater. Sci. Eng. C* **112**, 110900 (2020).
39. Gao, J., Gu, H. & Xu, B. Multifunctional magnetic nanoparticles: Design, synthesis, and biomedical applications. *Acc. Chem. Res.* **42**, 1097–1107 (2009).
40. Jamatia, R., Gupta, A. & Pal, A. K. Nano-FGT: A green and sustainable catalyst for the synthesis of spirooxindoles in aqueous medium. *RSC Adv.* **6**, 20994–21000 (2016).
41. Elinson, M. N., Ryzhkov, F. V., Zaimovskaya, T. A. & Egorov, M. P. Solvent-free multicomponent assembling of isatins, malononitrile, and dimedone: Fast and efficient way to functionalized spirooxindole system. *Monatshefte für Chemie-Chemical Monthly* **147**, 755–760 (2016).
42. Mamaghani, M., Tabatabaieian, K., Pourshiva, M. & Nia, R. H. Rapid and efficient synthesis of spiro-oxindoles using Fe₃+montmorillonite under ultrasonic irradiation. *J. Chem. Res.* **39**, 314–317 (2015).
43. Keshavarz, M. Ion-pair immobilization of l-prolinate anion onto cationic polymer support and a study of its catalytic activity for one-pot synthesis of spiroindolones. *J. Iran. Chem. Soc.* **13**, 553–561 (2016).
44. Baharfar, R. & Azimi, R. Immobilization of 1, 4-diazabicyclo [2.2. 2] Octane (DABCO) over mesoporous silica SBA-15: An efficient approach for the synthesis of functionalized spirochromenes. *Synth. Commun.* **44**, 89–100 (2014).
45. Goli-Jolodar, O., Shirini, F. & Seddighi, M. Introduction of a novel basic ionic liquid containing dual basic functional groups for the efficient synthesis of spiro-4H-pyrans. *J. Mol. Liq.* **224**, 1092–1101 (2016).

46. Mohamadpour, F., Maghsoodlou, M. T., Lashkari, M., Heydari, R. & Hazeri, N. Synthesis of quinolines, spiro [4 H-pyran-oxindoles] and xanthenes under solvent-free conditions. *Org. Prep. Proced. Int.* **51**, 456–476 (2019).
47. Nagaraju, S., Paplal, B., Sathish, K., Giri, S. & Kashinath, D. Synthesis of functionalized chromene and spirochromenes using l-proline-melamine as highly efficient and recyclable homogeneous catalyst at room temperature. *Tetrahedron Lett.* **58**, 4200–4204 (2017).
48. Moradi, L., Ataei, Z. & Zahraei, Z. Convenient synthesis of spirooxindoles using SnO₂ nanoparticles as effective reusable catalyst at room temperature and study of their in vitro antimicrobial activity. *J. Iran. Chem. Soc.* **16**, 1273–1281 (2019).
49. Wagh, Y. B., Padvi, S. A., Mahulikar, P. P. & Dalal, D. S. CsF promoted rapid synthesis of spirooxindole-pyran annulated heterocycles at room temperature in ethanol. *J. Heterocycl. Chem.* **57**, 1101–1110 (2020).
50. Chandam, D. R., Mulik, A. G., Patil, D. R. & Deshmukh, M. B. Oxalic acid dihydrate: Proline as a new recyclable designer solvent: A sustainable, green avenue for the synthesis of spirooxindole. *Res. Chem. Intermed.* **42**, 1411–1423 (2016).
51. Wang, G. D., Zhang, X. N. & Zhang, Z. H. One-pot three-component synthesis of spirooxindoles catalyzed by hexamethylenetetramine in water. *J. Heterocycl. Chem.* **50**, 61–65 (2013).
52. Meshram, H. M., Kumar, D. A., Prasad, B. R. V. & Goud, P. R. Efficient and convenient polyethylene glycol (PEG)-mediated synthesis of spiro-oxindoles. *Helv. Chim. Acta* **93**, 648 (2010).
53. Baghernejad, M., Khodabakhshi, S. & Tajik, S. Isatin-based three-component synthesis of new spirooxindoles using magnetic nano-sized copper ferrite. *New J. Chem.* **40**, 2704–2709 (2016).
54. Kidwai, M., Jahan, A. & Mishra, N. K. Gold (III) chloride (HAuCl₄·3H₂O) in PEG: A new and efficient catalytic system for the synthesis of functionalized spirochromenes. *Appl. Catal. A* **425**, 35–43 (2012).
55. Padvi, S. A., Tayade, Y. A., Wagh, Y. B. & Dalal, D. S. [bmim] OH: An efficient catalyst for the synthesis of mono and bis spirooxindole derivatives in ethanol at room temperature. *Chin. Chem. Lett.* **27**, 714–720 (2016).
56. Khot, S. S., Anbhule, P. V., Desai, U. V. & Wadgaonkar, P. P. Tris-hydroxymethylaminomethane (THAM): An efficient organocatalyst in diversity-oriented and environmentally benign synthesis of spirochromenes. *C. R. Chim.* **21**, 814–821 (2018).
57. Brahmachari, G. & Banerjee, B. Facile and chemically sustainable one-pot synthesis of a wide array of fused O- and N-heterocycles catalyzed by trisodium citrate dihydrate under ambient conditions. *Asian J. Organic Chemistry* **5**, 271–286 (2016).
58. Allahresani, A., Taheri, B. & Nasser, M. A. A green synthesis of spirooxindole derivatives catalyzed by SiO₂@gC₃N₄ nanocomposite. *Res. Chem. Intermed.* **44**, 1173–1188 (2018).
59. Dangelani, S. K., Panahi, F., Nourisefat, M. & Khalafi-Nezhad, A. 4-Dialkylaminopyridine modified magnetic nanoparticles: As an efficient nano-organocatalyst for one-pot synthesis of 2-amino-4 H-chromene-3-carbonitrile derivatives in water. *RSC Adv.* **6**, 92316–92324 (2016).
60. Mohammadfam, Y., Heris, S. Z. & Khazini, L. Experimental investigation of Fe₃O₄/hydraulic oil magnetic nanofluids rheological properties and performance in the presence of magnetic field. *Tribol. Int.* **142**, 105995 (2020).
61. Lai, L., Xie, Q., Chi, L., Gu, W. & Wu, D. Adsorption of phosphate from water by easily separable Fe₃O₄@ SiO₂ core/shell magnetic nanoparticles functionalized with hydrous lanthanum oxide. *J. Colloid Interface Sci.* **465**, 76–82 (2016).
62. Rezaei, F., Amrollahi, M. A. & Khalifeh, R. Design and synthesis of Fe₃O₄@ SiO₂/aza-crown ether-Cu (II) as a novel and highly efficient magnetic nanocomposite catalyst for the synthesis of 1, 2, 3-triazoles, 1-substituted 1H-tetrazoles and 5-substituted 1H-tetrazoles in green solvents. *Inorg. Chim. Acta* **489**, 8–18 (2019).
63. Nasser, M. A., Hemmat, K. & Allahresani, A. Synthesis and characterization of Co (III) salen complex immobilized on cobalt ferrite-silica nanoparticle and their application in the synthesis of spirooxindoles. *Appl. Organomet. Chem.* **33**, 4743 (2019).

Author contributions

S.G.A. Investigated and carried out the experiment. M.E. wrote the original draft; drew figures; reviewed the manuscript. Z.D. data collection, S.J. Conceptualization (lead); supervised the project; edited and reviewed the manuscript.

Competing interests

The authors declare no competing interests.

Additional information

Supplementary Information The online version contains supplementary material available at <https://doi.org/10.1038/s41598-022-10102-5>.

Correspondence and requests for materials should be addressed to S.J.

Reprints and permissions information is available at www.nature.com/reprints.

Publisher's note Springer Nature remains neutral with regard to jurisdictional claims in published maps and institutional affiliations.



Open Access This article is licensed under a Creative Commons Attribution 4.0 International License, which permits use, sharing, adaptation, distribution and reproduction in any medium or format, as long as you give appropriate credit to the original author(s) and the source, provide a link to the Creative Commons licence, and indicate if changes were made. The images or other third party material in this article are included in the article's Creative Commons licence, unless indicated otherwise in a credit line to the material. If material is not included in the article's Creative Commons licence and your intended use is not permitted by statutory regulation or exceeds the permitted use, you will need to obtain permission directly from the copyright holder. To view a copy of this licence, visit <http://creativecommons.org/licenses/by/4.0/>.

© The Author(s) 2022